Chapter 11. Oils and Surfactants

Werner Alpers
Institut für Meereskunde Universität Hamburg, Hamburg, Germany

Heidi A. Espedal
Nansen Environmental and Remote Sensing Center, Bergen, Norway

11.1 Introduction

Pollution of the sea surface by mineral or petroleum oil is a major environmental problem. Increased public pressure has forced national and international organizations to set up effective legislative protection of the marine and coastal environment over the last 15 to 20 years. As a result, many countries have signed the International Convention for the Prevention of Pollution from Ships (MARPOL 73/78) which sets standards for ship discharges, allowing discharges only beyond certain distances from the nearest coast and only at very small amounts. Several sea areas have been declared as Special Areas, where ship discharges are prohibited almost completely. Such Special Areas are the Mediterranean Sea, the Baltic Sea, and the North Sea. However, despite the MARPOL convention, large quantities of mineral oil are still being discharged from ships in these Special Areas.

Mineral oil floating on the sea surface does not always originate from ships. Other sources are refineries, oil terminals, industrial plants, oil platforms and seepage of natural oil from the sea bottom [*Espedal and Johannessen,* 2000]. It is estimated that 0.25% of world oil production ends up in the ocean. However, the main contribution of oil pollution originating from transportation activities still originates not from ship accidents, but from routine ship operations like tank washing and engine effluent (mostly sludge) discharges [*Lean and Hinrichsen,* 1992].

Synthetic aperture radar (SAR) images acquired by the ERS-1, ERS-2 and RADARSAT-1 satellites have been used extensively for obtaining statistical information on oil pollution [e.g. *Lu et al*., 1999, 2000, *Gade and Alpers*, 1999]. In particular, satellite images are very useful in locating the preferred areas ("hot spots") where tankers are washed and/or engine room effluents are discharged. In a study by *Pavlakis et al.* [2001], 1600 satellite SAR images from the Mediterranean Sea were analyzed. The study revealed the dramatic extent of oil pollution originating from ships in this sea area, which is designated a Special Area according to the MARPOL convention.

Satellite SAR imagery can also be used for monitoring oil pollution in coastal waters [*Wahl et al*., 1996]. ERS SAR imagery has been successfully adopted in an operational oil spill monitoring service performed by Kongsberg Satellite Services, KSAT (formerly Tromsø Satellite Station) in Norway [*Pedersen et al*., 1996]. The researchers use the SAR imagery acquired by satellites (ERS, RADARSAT-1 and ENVISAT) to locate potential oil spills. Information on high probability spills can immediately be sent by fax to the Norwegian Coast Guard, which may then redirect a monitoring aircraft for further investigations. The service is also currently in use for Denmark, Sweden, Finland and the Netherlands. A demonstration phase is also operating in Germany, England and Scotland.

Mineral oil floating on the sea surface becomes visible on radar images because it damps

the short gravity-capillary waves that are responsible for the radar backscattering. Real aperture radars (RARs) as well as synthetic aperture radars (SARs) used for monitoring coastal waters for oil pollution usually operate at incident angles between 20 and 70 degrees, i.e., at incident angles where the radar backscattering can be described by Bragg scattering theory [e.g., *Valenzuela*, 1978]. According to Bragg theory, the backscattered radar power is proportional to the spectral energy density of those short ocean waves which propagate toward or away from the look direction of the radar antenna and which have wavelength $\lambda_B = \lambda_0 / 2\sin\theta$, where λ_0 is the radar wavelength and θ the incident angle (the angle between nadir and look direction of the antenna). These waves are called Bragg waves and have wavelengths in the centimeter to decimeter range. A precondition for detecting mineral oil spills on the sea surface is that the wind is strong enough for generating Bragg waves. For X- and C-band radars operating at wavelengths between 3 cm and 5 cm, and between 5 cm and 7 cm, respectively, the threshold for generating Bragg waves lies between 2 and 3 ms^{-1}. According to Bragg scattering theory, lower frequency radars respond to longer surface waves. Since the damping of the Bragg resonant waves is more efficient at shorter wavelength, X- and C-band radars are more efficient in detecting oil films than L- or P-band radars operating at wavelengths between 19 cm and 77 cm, and between 77 cm and 133 cm, respectively. This efficiency has been confirmed in several experiments [*Johannessen et al.,* 1995, *Gade et al.,* 1998]. The ERS, RADARSAT-1 and ENVISAT satellites all carry C-band SAR systems. However, while the ERS SAR uses VV polarization, RADARSAT-1 SAR uses HH polarization, and the new ENVISAT SAR, called ASAR (which stands for Advanced SAR), has an alternating polarization capability (HH, VV and cross-polarization). According to radar theory, VV polarization gives higher radar backscatter from the sea surface than HH polarization because of the large dielectric constant of the ocean surface [*Elachi,* 1988]. Thus, VV polarized radars will provide more contrast (better signal-to-background ratio) when oil is floating on the sea surface. VV is therefore the preferred polarization for detecting oil pollution at sea.

In addition to the low wind detection threshold, there is also a maximum wind speed above which oil films become undetectable by radar. At high wind speed the damping effect can disappear in the background noise of wind-generated waves [*Demin et al.,* 1985], and at higher wind speed the oil disappears from the sea surface because it is washed down by breaking waves [*Scott,* 1986, *Espedal and Wahl,* 1999]. Depending on the type of the oil and the thickness of the oil film, oil films become undetectable at wind speeds between 10 ms^{-1} and 14 ms^{-1}.

In addition to mineral oil, surface films of natural origin floating on the sea surface (called biogenic slicks) damp the short gravity-capillary waves [*Lucassen,* 1982; *Huehnerfuss et al.,* 1983, 1987, *Alpers and Huehnerfuss*, 1989]. Biogenic slicks are produced by marine plants and animals and are frequently encountered on the sea surface, especially during plankton bloom seasons [*Espedal et al.,* 1996, 1998]. The frequent presence of biogenic slicks often makes it difficult to decide whether the dark patches visible on radar images of the sea surface (or, more accurately, the sea areas of reduced radar backscatter relative to the surrounding areas) originate from mineral oil spills or from biogenic slicks.

To make things even more difficult, dark patches on radar images of the sea surface can also be caused by (1) turbulence generated in the water by the propeller of a ship, (2) rain impinging on the sea surface, and (3) grease ice floating on the water. These phenomena also damp the short gravity-capillary waves and thus reduce the backscattered radar power at intermediate incident angles where radar backscattering can be described by Bragg scattering theory. Furthermore, dark patches can also result from reduced wind speed as encountered, e.g., in the wind shadow behind islands or coastal mountains. Alternatively, they can result from

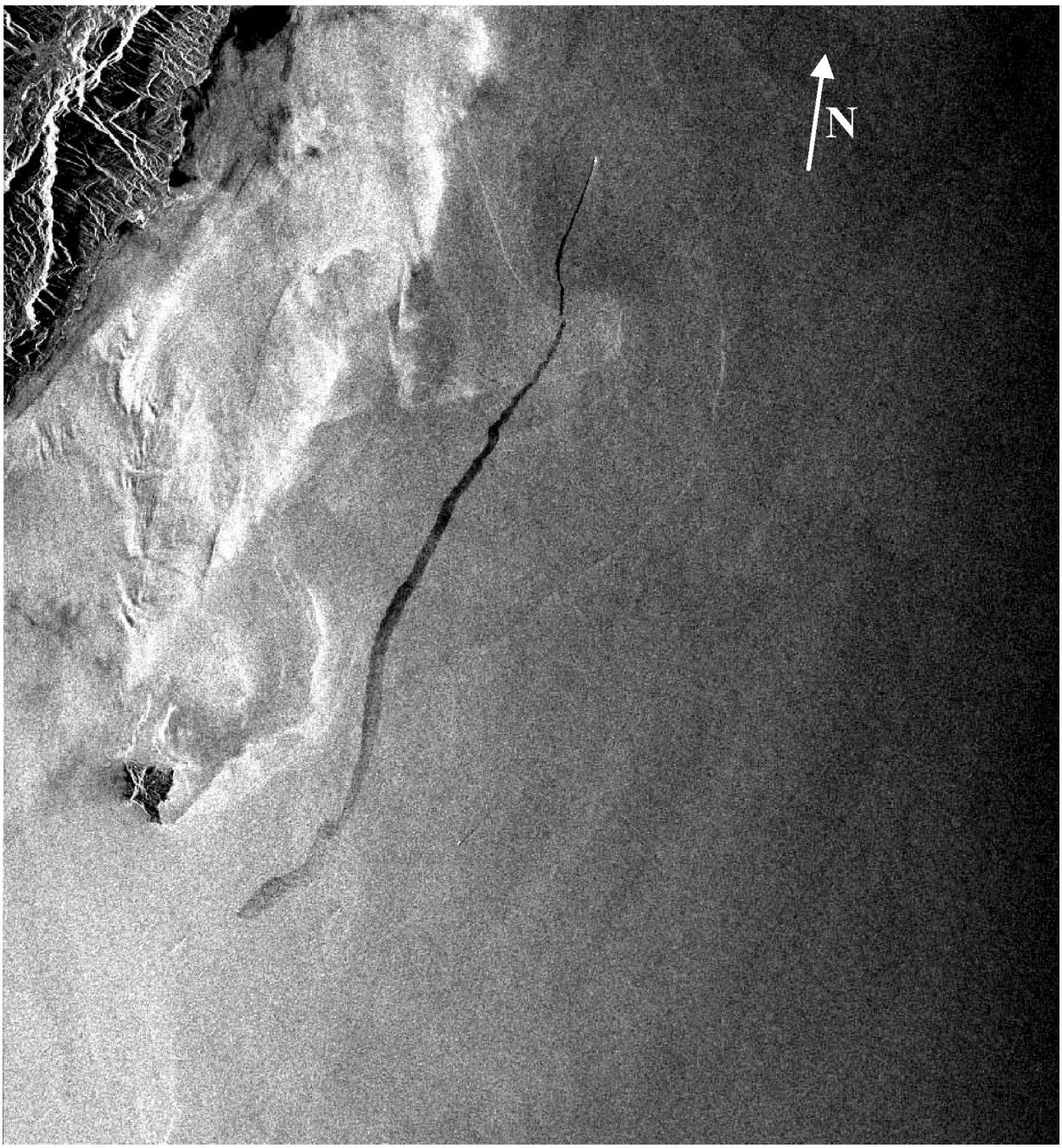

Figure. 11.1. A ship traveling northward (bright spot at the front of the black line) discharging oil. The oil disperses with time causing the oil trail to widen. The oil trail is more than 80 km long. This ERS-1 (C-band, VV) SAR image was acquired on 20 May 1994 at 1420 UTC over the Pacific Ocean, east of Taiwan (orbit 14874, frame 2364, frame center 23°01'N, 121°41'E). The imaged area is 100 km x 100 km. ©ESA 1994.

reduced wind stress due to colder sea surface temperatures as encountered, e.g., in upwelling regions or in cold plumes of river outflows. The colder water often changes the stability of the air-sea interface. If the water is colder than the air above, then the air-sea interface is stable and it takes a higher wind speed to generate small-scale sea surface roughness (Bragg waves) than in the case of a neutral interface (water temperature is equal to the air temperature) or an unstable

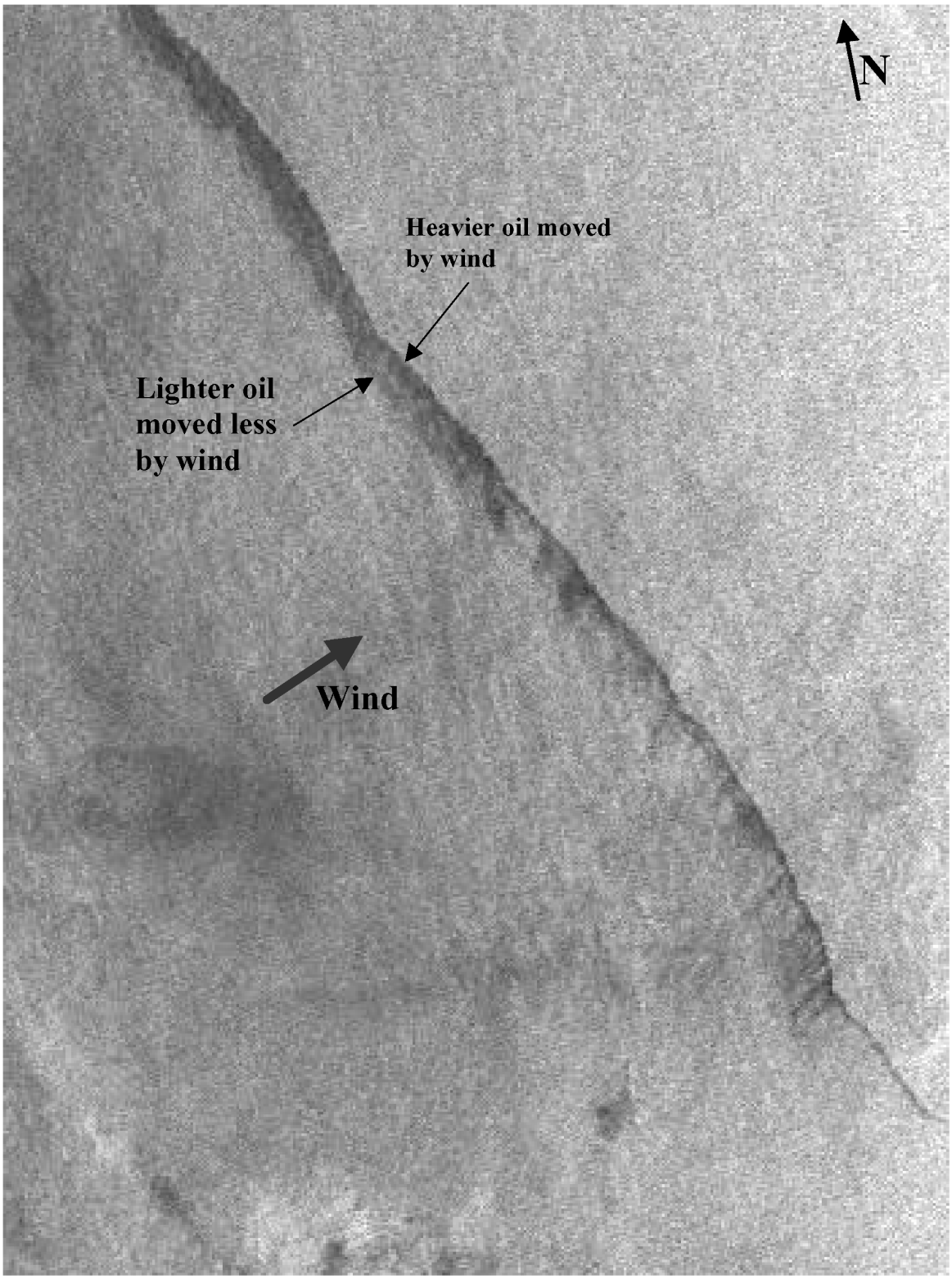

Figure 11.2. Section of an ERS-2 (C-band, VV) SAR image from the Indian Ocean acquired 6 April 1999 at 0458 UTC (orbit 20700, frame 3393, frame center 10°36'N, 81°49'E) showing a "feathered" structure of an oil trail. Wind causes the heavy components of the mineral oil film accumulate at the downwind side (dark line in the image). The "feathered" side is always located upwind. The wind direction arrow in the image was obtained from the modeled surface wind field provided by the European Centre for Medium-range Weather Forecasts (ECMWF). ©ESA 1999.

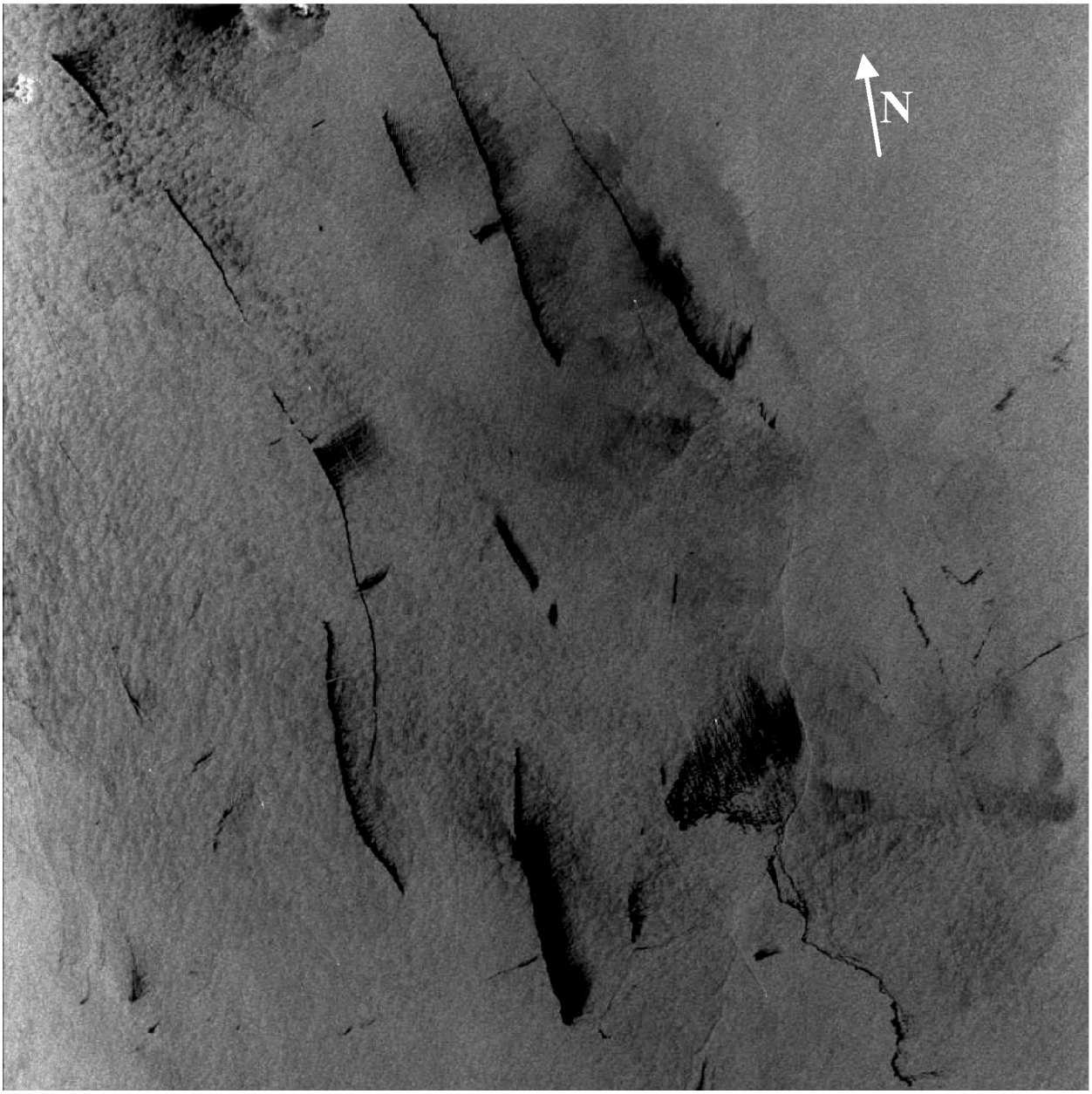

Figure 11.3. Oil polluted sea area in a busy shipping lane off the coast of Malaysia (near Kuantan). The wind blows from an easterly direction causing the feathering of oil trails. This ERS-2 (C-band, VV) SAR image was acquired on 4 April 1997 at 0325 UTC over the South China Sea (orbit 10221, frame 3519, frame center 4°20'N, 103°59'E). The imaged area is 100 km x 100 km. ©ESA 1997.

interface (water temperature is higher than the air temperature). Thus we conclude that it is often difficult to identify unambiguously mineral oil floating on the sea surface by associating them with areas of reduced radar backscatter in radar images (dark areas in the SAR image or areas that are darker than the surrounding area). However, some algorithms have been developed to minimize the risk of false classification of oil patches in SAR imagery, see, e.g., *Espedal et al.* [1998] or *Fiscella et al.* [2000]. These algorithms are based on various parameters calculated from dark areas in radar images, but may also include contextual information such as wind (or wind history), current, bathymetry, and location of potential pollution sources.

11.2. Mineral oil films

As stated before, not all mineral oil encountered at the sea surface originates from ships. But if the oil originates from moving ships, then the identification on radar images is much easier. In general, ships discharge oily effluents en route, leaving behind the ship linear-shaped spills or trails. When oil is discharged in a current-free and calm sea, the resulting overall spill geometry will follow the route of the ship. Automatic oil detection techniques often use this linearity for identifying such oil spills. However, when the ship is maneuvering or when a non-uniform surface current is present, then the contour of the spill can deviate significantly from linearity [*Ochadlick et al*., 1992]. When oil is discharged from a moving ship, it will also spread laterally, resulting in an oil trail whose width increases with distance from the ship (see Figure 11.1). Typical spreading rates were found to be proportional to time raised to the 0.6 power ($t^{0.6}$). During their fate in the sea, mineral oil films are subject to spreading (by the action of wind and currents), evaporation of lighter chemical components, dispersion (mixing with seawater), emulsification, dissolution, oxidation, sedimentation, and biodegradation [*Jordan and Payne*, 1980]. Thus, after some time, oil slicks become undetectable on radar images of the sea surface. The time at which oil slicks become undetectable depends on the type, quantity, and thickness of the oil and on environmental conditions. The stronger the wind, the shorter the time oil slicks persist on the sea surface [*Espedal and Wahl*, 1999]. The time of persistence usually varies between a few days and several weeks.

Winds (especially high winds) strongly affect the shape of an oil trail behind a ship. Directly, through accumulating the majority of the spill in its downwind side, but also through generating a "feathered" trail structure. The feathering is caused by vortices known as Langmuir circulation which split the spill into streaks [*Pavlakis et al*., 2001, *Langmuir,* 1938]. The feathered side is usually the upwind side (Figure 11.2). To the non-expert, this may seem to be counter-intuitive. But it has been experimentally verified that, at most wind and wave conditions, the heavy constituents of an oil spill are moved faster by the wind (the wind drift) than the lighter constituents are. Furthermore, several radar images of feathered oil trails with collocated wind information have confirmed this behavior.

In addition to Figure 11.1, more examples of radar images acquired by the C-band (5.3 GHz) synthetic aperture radar aboard the European Remote Sensing satellites ERS-1 and ERS-2 over ocean areas polluted by mineral oil films are shown in Figures 11.3 through 11.5.

Figure 11.3 shows a large number of oil trails having various shapes in a busy shipping lane in South East Asia. In the case of fresh oil spills, the direction of the ships can be inferred to be opposite of the direction in which the oil trails widen. This is the case for the three large oil trails visible in the northern section of Figure 11.3. From the "feathered" shape of the oil trails, it can be inferred that the wind was blowing from a northeasterly direction. The large oil spills visible in the southern section of the image are apparently older than the ones in the northern section.

Many of the black patches visible in Figure 11.4 likely do not originate from ship discharges, but rather from natural oil seeps, which are known to exist in this area. The oil seeps at the ocean bottom are stationary, but the position of the oil patches on the sea surface varies according to the oceanic and meteorological conditions. Thus by repeatedly taking SAR images over the same ocean area and taking into account the advection of the oil films by ocean currents and by wind drift, the position of oil seeps can be determined. This method of detection is widely used by oil companies in offshore oil prospecting.

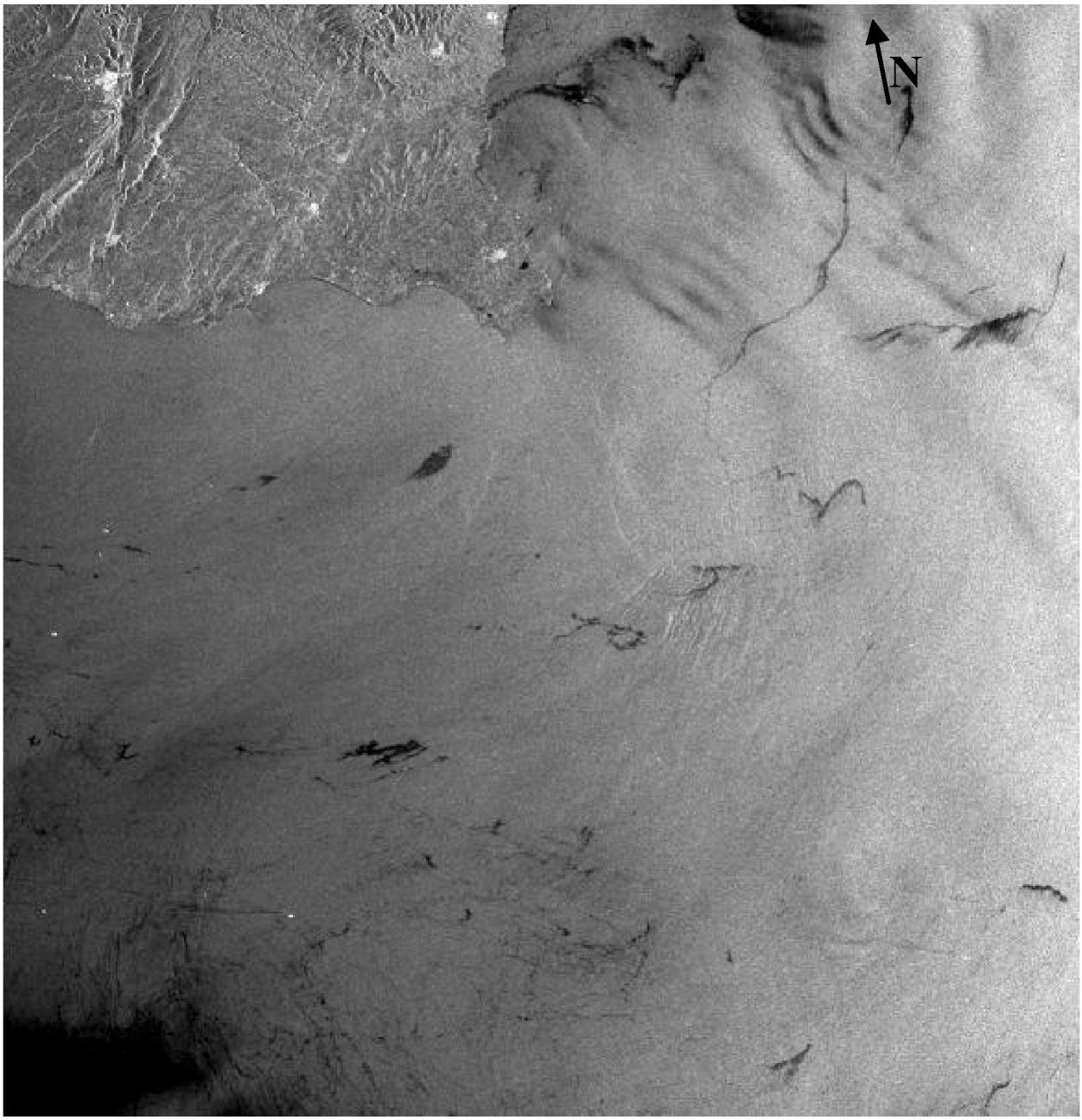

Figure 11.4. Area of the Mediterranean Sea located off the southeast coast of Sicily (Italy). Some of the dark patches visible on this image are very likely due to oil slicks originating from natural oil seeps that are known to exist in this area. If dark patches are found repeatedly at approximately the same location at the sea surface and if they do not have the characteristic linear shape of a ship-generated oil spill, then one may suppose that they originate from natural oil seeps. This ERS-1 (C-band, VV) SAR image was acquired on 26 May 1994 at 0941 UTC (orbit 14957, frame 2871, frame center 36°28'N, 15°04'E). The imaged area is 100 km x 100 km. ©ESA 1994.

Figure 11.5 shows a cluster of oil rigs (the bright dots) in the Caspian Sea east of Baku surrounded by oil slicks. These oil rigs are quite old and it is well known that they leak a large amount of oil into the sea. In other cases, black slicks connected to oil platforms may be caused by drilling mud or drain water and may contain only small amounts of oil.

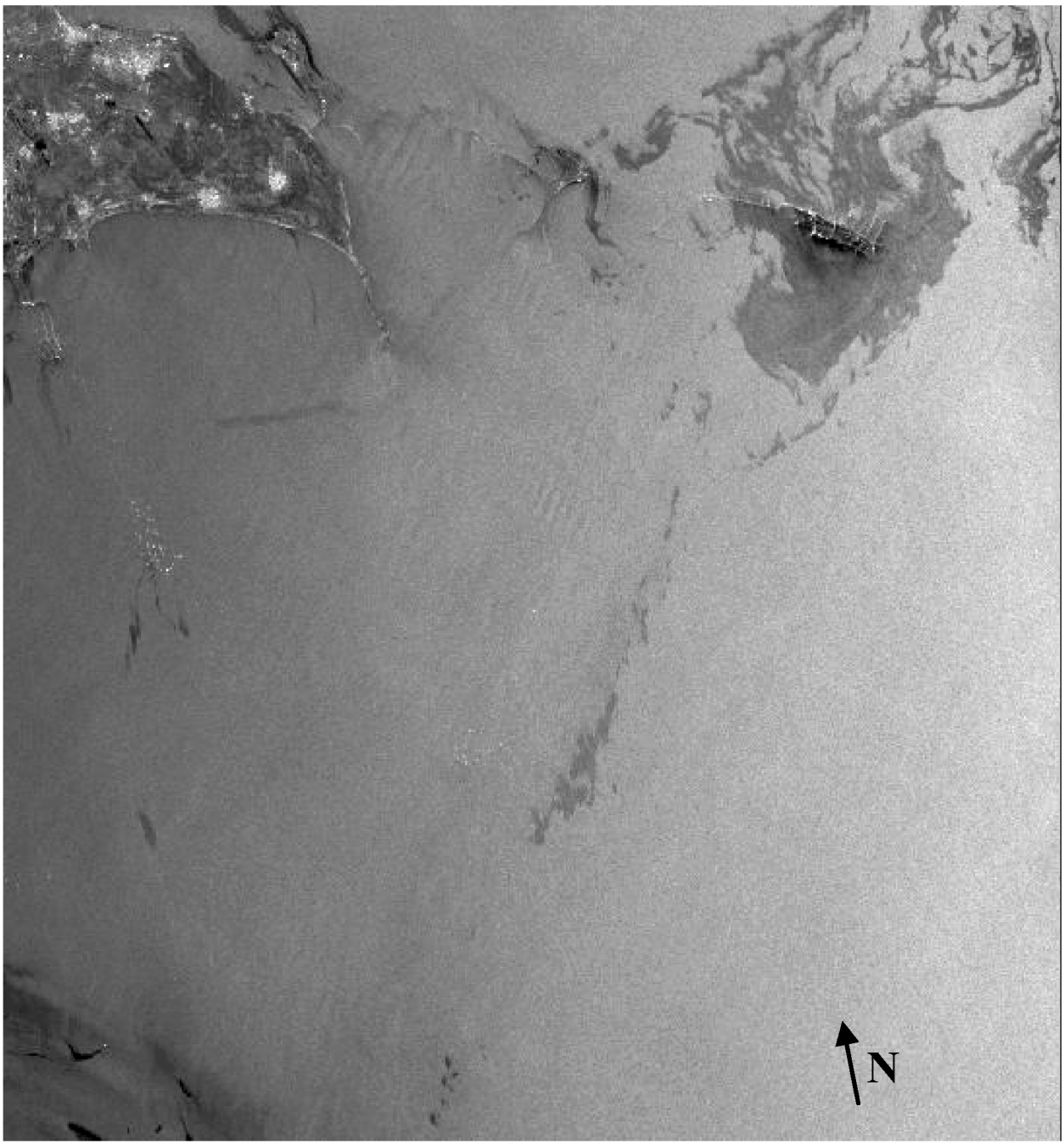

Figure 11.5. A cluster of oil rigs (bright dots) in the Caspian Sea surrounded by oil slicks is visible in the upper right-hand corner of the image. The imaged area is located east of Baku, Azerbaidzan. This ERS-1 (C-band, VV polarization) SAR image was acquired on 12 May 1996 at 0723 UTC (orbit 25230, frame 2799, frame center 40°04'N, 50°27'E). The imaged area is 100 km x 100 km. ©ESA 1996.

11.3. Biogenic slicks

Biogenic slicks are natural surface films that consist of surface-active compounds that originate from marine plants or animals. Surface-active compounds are substances that, according to their chemical structure, accumulate at the water-air boundary. The composition of biogenic slicks varies, but substances such as proteins, lipids, organic acids, saccharides and

Figure 11.6. Area of the Baltic with the German island of Fehmarn (in the center) and the Danish island of Lolland (in the upper right-hand section). The sea area is partly covered with biogenic slicks that are abundant at this time of the year because of the spring plankton bloom in the Baltic Sea. The slicks act as tracers for the surface currents associated with eddies and thus render them visible on the SAR image. This ERS-2 (C-band, VV) SAR image was acquired on 10 May 1998 at 2115 UTC over the Baltic Sea (orbit 15972, frame 1098, frame center 54°28'N, 11°13'E). The imaged area is 100 km x 100 km. ©ESA 1998.

metals associated with the organic matter are usually present at higher concentrations than in the corresponding bulk water [*Duce et al.,* 1994]. In general, the biogenic surface slicks consisting of sufficiently hydrophobic substances are only one molecular layer thick (approximately 3 nm). This implies that only a few liters of surface-active material are needed to cover an area of 1 km^2. The prime biological producers of natural surface films in the sea are algae and some

Figure 11.7. Biogenic slicks in the Caspian Sea south of the Volga estuary. This is an area of high eutrophication because of the high input of nutrients from the Volga river. The surface features visible on this image very likely result from wind-induced surface currents. This ERS-2 (C-band, VV) SAR image was acquired on 12 October 1993 at 1854 UTC (orbit 11724, frame 0891, frame center 44°45'N, 49°03'E). The imaged area is 100 km x 100 km. ©ESA 1993.

bacteria. In addition, zooplankton and fish produce surface-active materials, but the amount is usually small in comparison with the primary biological producers. Primary production depends on the quantity of light energy available to the organism and on the availability of inorganic nutrients. In the higher latitudes, light energy depends strongly on the season of the year. This results in a seasonal variation of the primary biological production in the ocean and thus of the

Figure 11.8. An example of natural film damping the ocean surface waves. The edges of the slick are clearly delineated along the center of the photograph. The small slick sampler device seen in the bottom left corner of the photograph took samples that confirmed presence of natural film in the damped region [*Espedal et al.*, 1996].

coverage by biogenic slicks. At times when the biological productivity is high, i.e., during plankton blooms, the probability of encountering natural biogenic surface films is strongly enhanced.

The area extent, the concentration, and the composition of the surface films vary strongly with wind and sea conditions and with time. At high wind speeds (typically above 7 to 10 ms^{-1}) the surface film disappears from the sea surface because of entrainment into the underlying water by wave breaking. The Bragg waves are no longer damped and thus the surface films become undetectable by radar. In general, the probability of encountering surface films of biogenic origin decreases with increasing wind speed. This is because the higher the waves, the more the surface films are removed from the sea surface, mainly by wave breaking, including micro-breaking. Furthermore, after the passage of storms when the wind has calmed down, enhanced coverage of the sea surface with biogenic slicks is often observed. This is because the amount of surface-active material released by plankton into the water increases during high wind speed periods, and because the surface-active substances are being transported to the sea surface by turbulence and rising air bubbles generated by breaking waves. The composition of biogenic slicks also varies with time because dissolution, evaporation, enzymatic degradation, and photocatalytic oxidation selectively remove constituents of the surface films. Examples of large sea areas covered with natural surface films are shown in Figures 11.6 and 11.7. Because surface films tend to accumulate along convergence zones of current systems and spread out in divergent zones, they render surface current patterns visible on radar images as evident in Figures 11.6 and 11.7 [*Johannessen et al.,* 1996]. Figure 11.8 shows a photograph of natural film damping surface waves.

The image depicted in Figure 11.6 shows an area of the western Baltic Sea between Germany and Denmark. This ERS-2 SAR image was acquired at the peak of the spring plankton bloom season when large parts of the Baltic Sea are covered with biogenic slicks. Since the sea surface is only partially covered by biogenic slicks, surface current features, in particular eddies, become visible on this radar image because the surface current re-distributes the slick material and, thus, the slicks act as tracers for the surface current field.

Figure 11.7 shows a similar image from the Caspian Sea. The imaged area is located south of the mouth of the river Volga. This river carries a heavy load of pollutants originating from fertilizers that are washed out from agricultural fields, but also originating from industrial and municipal plants. The pollutants serve as nutrients for marine organisms that experience a rapid growth that leads to enhanced generation of biogenic slicks. The oceanic eddies in Figure 11.7 are very likely wind-induced. The most remarkable feature on this image is the mushroom-like feature consisting of two counter-rotating eddies.

11.4 References:

Alpers, W., and H. Hühnerfuss, 1989: The damping of ocean waves by surface films: A new look at an old problem. *J. Geophys. Res*., 94, 6251–6265.

Demin, B. T., S. A. Ermakov, N. Y. Pelinovsky, T. G. Talipova, and A. I. Sheremet'yeva, 1985: Study of the elastic properties of sea surface-active films. *Atmos. Oceanic Phys*., 21, 312–316.

Duce, R., and Coauthors, 1994: The sea-surface microlayer and its potential role in global change. GESAMP WG 34, XXIV/7, A&M University Press, College Station, TX, 100 pp.

Elachi, C., 1988: *Spaceborne Radar Remote Sensing: Applications and Techniques*. ISBN 0-87942-241-6, IEEE press, 288 pp.

Espedal, H. A. and T. Wahl, 1999: Satellite SAR oil spill detection using wind history information. *Int. J. Remote Sens.*, 20, 49–65.

——, and O. M. Johannessen, 2000: Detection of oil spills near offshore installations using synthetic aperture radar (SAR). *Int. J. Remote Sens.*, 21, 2141–2144.

——, ——, and J. Knulst, 1996: Natural films in coastal waters. *Geophys. Res. Lett.*, 23, 3151–3154.

——, ——, J. A. Johannessen, E. Dano, D. R. Lyzenga, and J. C. Knulst, 1998: COASTWATCH'95: ERS 1/2 SAR detection of natural film on the ocean surface. *J. Geophys. Res.*, 10, 24 969–24 982.

Fiscella, B., A. Giancaspro, F. Nirchio, P. Pavese, and P. Trivero, 2000: Oil spill detection using marine SAR images. *Int. J. Remote Sens*., 21, 3561–3566.

Gade, M., and W. Alpers, 1999: Using ERS-2 SAR for routine observation of marine pollution in European coastal waters. *Sci. Total Environ*., 237–238, 441–448.

——, ——, H. Hühnerfuss, H. Masuko, and T. Kobayashi, 1998: Imaging of biogenic and anthropogenic ocean surface films by the multifrequency/multipolarization SIR-C/X-SAR. *J. Geophys. Res.*, 103, 18 851–18 866.

Huehnerfuss, H., W. Alpers, W. D. Garrett, P. A. Lange, and S. Stolte, 1983: Attenuation of capillary and gravity waves at sea by monomolecular organic surface films. *J. Geophys. Res.*, 88, 9809–9816.

——, W. Walter, P. A. Lange, and W. Alpers, 1987: Attenuation of wind waves by monomolecular sea slicks and the Marangoni effect. *J. Geophys. Res.*, 92, 3961–3963.

Johannessen, J. A., D. R. Lyzenga, R. Shuchman, H. A. Espedal, and B. Holt, 1995: Multifrequency SAR observations of ocean surface features off the coast of Norway. *Proc. IGARSS'95*, Florence, Italy, IEEE, 1328–1330.

——, R. A. Shuchman, G. Digranes, D. R. Lyzenga, C. Wackerman, O. M. Johannessen, and P. W. Vachon, 1996: Coastal ocean fronts and eddies imaged with ERS 1 Synthetic Aperture Radar. *J. Geophys. Res.*, 101 (C3), 6651–6667.

Jordan, R. E., and J. R. Payne, 1980: *Fate and Weathering of Petroleum Spills in the Marine Environment*. Ann Arbor Science, 174 pp.

Langmuir, I., 1938: Surface motion induced by the wind. *Science*, 87, 119–123.

Lean, G., and D. Hinrichen, 1999: *WWF Atlas of the Environment*. Helicon Publishing, 192 pp.

Lu, J., H. Lim., S. C. Liew, M. Bao, and L. K. Kwoh, 1999: Statistics in Southeast Asian waters compiled from ERS synthetic aperture radar imagery. *Earth Observation Quart.,* 621, 13–17.

Lu, J., L. K. Kwoh, H. Lim, S. C. Liew, and M. Bao, 2000: Mapping oil pollution from space. *Backscatter*, 11, 23–26.

Lucassen, J., 1982: Effect of surface-active material on the damping of gravity waves: A reappraisal. *J. Colloid Interface Sci*., 85, 52–58.

Ochadlick, A. R., P. Cho, and J. Evans-Morgis, 1992: Synthetic aperture radar observations of current colocated with slicks. *J. Geophys. Res.,* 97, 5325–5333.

Pavlakis, P., D. Tarchi, and A. J. Sieber, 2001: On the monitoring of illicit vessel discharges using spaceborne SAR remote sensing—A reconnaissance study in the Mediterranean Sea. *Ann. Telecommun.,* 56, 700–718.

Pedersen, J., L. Seljelv, G. D. Strøm, O. Follum, J. Andersen, T. Wahl, and Å. Skøelv, 1996: Oil spill detection by use of ERS SAR data: From research and development towards pre-operational early warning detection service. *Proc. Second ERS Application Workshop*, London, United Kingdom, ESA, Publ. SP-383, 181–185.

Scott, J. C., 1986: Surface films in oceanography. ONRL Workshop Report c-11-86, 19 pp.

Valenzuela, G. R., 1978: Theories for the interaction of electromagnetic and ocean waves—A review. *Bound.-Layer Meteor*., 13, 61–85.

Wahl, T., and Coauthors, 1996: Radar satellites: A new tool for pollution monitoring in coastal waters. *Coastal Management*., 24, 61–71.